


RESEARCH

Open Access

5'-tRF-GlyGCC: a tRNA-derived small RNA as a novel biomarker for colorectal cancer diagnosis



Yingmin Wu^{1†}, Xiangling Yang^{2,3†}, Guanmin Jiang^{4†}, Haisheng Zhang¹, Lichen Ge⁵, Feng Chen¹, Jiexin Li^{1*}, Huanliang Liu^{2,3*} and Hongsheng Wang^{1*} 

Abstract

Background: tRNA-derived small RNAs (tDRs), which are widely distributed in human tissues including blood and urine, play an important role in the progression of cancer. However, the expression of tDRs in colorectal cancer (CRC) plasma and their potential diagnostic values have not been systematically explored.

Methods: The expression profiles of tDRs in plasma of CRC and health controls (HCs) are investigated by small RNA sequencing. The level and diagnostic value of 5'-tRF-GlyGCC are evaluated by quantitative PCR in plasma samples from 105 CRC patients and 90 HCs. The mechanisms responsible for biogenesis of 5'-tRF-GlyGCC are checked by in vitro and in vivo models.

Results: 5'-tRF-GlyGCC is dramatically increased in plasma of CRC patients compared to that of HCs. The area under curve (AUC) for 5'-tRF-GlyGCC in CRC group is 0.882. The combination of carcinoembryonic antigen (CEA) and carbohydrate antigen 199 (CA199) with 5'-tRF-GlyGCC improves the AUC to 0.926. Consistently, the expression levels of 5'-tRF-GlyGCC in CRC cells and xenograft tissues are significantly greater than that in their corresponding controls. Blood cells co-cultured with CRC cells or mice xenografted with CRC tumors show increased levels of 5'-tRF-GlyGCC. In addition, we find that the increased expression of 5'-tRF-GlyGCC is dependent on the upregulation of AlkB homolog 3 (ALKBH3), a tRNA demethylase which can promote tRNA cleaving to generate tDRs.

Conclusions: The level of 5'-tRF-GlyGCC in plasma is a promising diagnostic biomarker for CRC diagnosis.

Keywords: 5'-tRF-GlyGCC, CRC, ALKBH3, Plasma, tRNA-derived small RNAs

* Correspondence: lijixin3@mail.sysu.edu.cn; liuhuan@mail.sysu.edu.cn; whongsh@mail.sysu.edu.cn

[†]Yingmin Wu, Xiangling Yang and Guanmin Jiang contributed equally to this work.

¹Guangdong Key Laboratory of Chiral Molecule and Drug Discovery, School of Pharmaceutical Sciences, Sun Yat-sen University, Guangzhou 510006, Guangdong, China

²Guangdong Provincial Key Laboratory of Colorectal and Pelvic Floor Diseases, Guangdong Institute of Gastroenterology, The Sixth Affiliated Hospital, Sun Yat-sen University, Guangzhou 510655, Guangdong, China
Full list of author information is available at the end of the article



© The Author(s). 2021 **Open Access** This article is licensed under a Creative Commons Attribution 4.0 International License, which permits use, sharing, adaptation, distribution and reproduction in any medium or format, as long as you give appropriate credit to the original author(s) and the source, provide a link to the Creative Commons licence, and indicate if changes were made. The images or other third party material in this article are included in the article's Creative Commons licence, unless indicated otherwise in a credit line to the material. If material is not included in the article's Creative Commons licence and your intended use is not permitted by statutory regulation or exceeds the permitted use, you will need to obtain permission directly from the copyright holder. To view a copy of this licence, visit <http://creativecommons.org/licenses/by/4.0/>. The Creative Commons Public Domain Dedication waiver (<http://creativecommons.org/publicdomain/zero/1.0/>) applies to the data made available in this article, unless otherwise stated in a credit line to the data.

Background

Colorectal cancer (CRC) is one of the most common cancers worldwide and the fourth leading cause of cancer-induced death [30]. The survival of CRC patients is mostly affected by the stage of disease at the time of diagnosis. The 5-year survival rate of patients diagnosed at the localized stage is reported to be 90%, while it is diagnosed to be 10% at the regional or distant stage [24]. Thus, early screening is quite necessary for improving the clinical outcome of patients. Currently, the early screening and diagnosis of CRC are mainly based on fiber-optic colonoscopy and fecal occult blood (OB) testing such as carcinoembryonic antigen (CEA) and carbohydrate antigen 199 (CA199) [6, 21]. Colonoscopy is invasive, painful, expensive, and unsafe for patients [23]. Due to insufficient sensitivity and organ specificity, the OB test mainly used to detect the recurrence of CRC [6]. Therefore, identifying a simple, non-invasive, and high-diagnostic efficacy biomarker is urgently needed for early CRC screening and diagnosis.

tRNA-derived small RNAs (tDRs) are fragments of precursor or mature tRNAs that are usually 14~50 nucleotides (nt) in length [17]. According to the location of biogenesis, tDRs can be generally grouped into tRNA halves and tRNA-derived small RNA fragments (tRFs) [31, 37]. Further, tRFs can be further classified into 3 sub-groups: 5'-tRF, 3'-tRF, and inter tRF (i-tRF) [16, 18]. They are functionally diverse and associated with the regulation of gene expression, RNA processing, ribosome biogenesis, and LTR-retrotransposons [15, 26, 42]. The dysregulation of tDRs is associated with various human diseases, such as cancer, virus infection, metabolic disorder, and neurodegenerative diseases [3, 15, 42]. tDRs are associated with cancer progression via increasing cell proliferation in breast and prostate cancers [11]. Our recent study indicated that tRNA demethylase AlkB Homolog 3 (ALKBH3) can promote cancer progression via induction of tDRs [4].

The tDRs have been detected in body fluids such as blood and urine since the 1970s [1, 35]. Increasing evidence confirms the presence of high-abundant tDRs in different types of human cell lines, tissues, or extracellular body fluids [8, 11, 28, 33]. Recently, tDRs have been reported to distinguish between pre- and post-seizure patients [10]. Consistently, emerging evidences indicated that tDRs might be used as potential biomarkers for certain types of cancer monitoring. For example, tDRs were dramatically increased in plasma exosomes of liver cancer patients, and four tDRs have the potential to become novel diagnostic biomarkers [41]. Circulating tDR-7816 expression is a novel potential biomarker for the diagnosis of patients with early non-triple-negative breast cancer [13].

In the present study, we investigated the expression profile of tDRs in plasma of CRC patients. The results showed that the level of 5'-tRF-GlyGCC is higher in CRC patients than in healthy controls (HCs) and highlighted that 5'-tRF-GlyGCC is a promising diagnostic biomarker for CRC patients. Its expression is positively correlated with ALKBH3 both *in vitro* and *in vivo*, respectively. Our results not only expand the distribution of non-coding RNAs in plasma, but also highlight the potential of tDRs as a promising biomarker for CRC diagnosis.

Methods

Human sample collection

Samples from 105 CRC patients and 95 HCs who had no history of basic or chronic diseases were collected from the Department of Clinical Laboratory of the Sixth Affiliated Hospital, Sun Yat-sen University, using tube for ethylene diamine tetraacetic acid (EDTA) anticoagulation. Unless otherwise stated, blood samples were centrifuged within 1 h of collection for 10 min at 3500 rpm at room temperature in a swing bucket centrifuge. Plasma samples were centrifuged at 13,000 r/min at 4 °C before the experiment. Separated plasma was transferred into a 1.5 mL RNase free polypropylene (PP) tube and stored at -80 °C until RNA isolation within three months. In addition, 3 CRC patients and 3 HC samples with the detail information provided in Table S1 were collected for small RNA sequencing. All CRC patients were diagnosed on the basis of histopathology by biopsy or endoscopic examination. Plasma samples were collected at the time of diagnosis without surgery, chemotherapy, radiation, or any other kinds of treatment.

In order to evaluate the correlation between the expression of 5'-tRFglyGCC in CRC tissues vs plasma of the same patients, 16-paired fresh tumor tissue and plasma were obtained from patients who underwent curative resection at the Sixth Affiliated Hospital, Sun Yat-sen University. None of the patients had received anticancer therapy before the sampling. Further, individuals with concurrent autoimmune disease, HIV, or syphilis were excluded.

The CRC stage was assessed by the TNM system according to the American Joint Committee on Cancer Staging Manual, Seventh Edition. Written informed consent was obtained from the patients. Ethic approval was obtained from the Ethics Committee of the Sixth Affiliated Hospital of Sun Yat-sen University (No. 2018ZSLYEC-008). Details of all samples are provided in Table S2.

Small RNA library preparation and sequencing

The small RNA library preparation and sequencing were conducted according to our previous study [4]. Briefly, total RNA from plasma of 3 CRC patients and 3 HCs were extracted with Trizol reagent (Invitrogen, Carlsbad,

CA, USA). Then, total RNAs were denatured and separated by a 15% TBE-Urea gel with 10/60 oligo length standard ladder (Integrated DNA Technologies, Coralville, IA). RNAs of 10 to 50 nt in gels were cut and recovered by small RNA PAGE recovery kit (Zymo Research, Irvine, CA, USA). After being treated with Tris for deacylation [8, 27] and T4 PNK for RNA end repair, the recovered tDRs were used for library preparation by use of NEB small RNA library preparation kit (E7330S). The purified libraries were quantified and validated. All 6 libraries were sequenced on an Illumina HiSeq 2500 (Illumina, San Diego, CA, USA).

Quantitative real-time PCR

Total RNA from cell was isolated using TRIzol (Takara). The yield and purity of RNA were measured by Nano-Drop 2000 (Thermo Fisher). cDNA was generated using the PrimeScript™ RT Master Mix (Takara) and small RNA first-strand was generated using the Mir-X™ miRNA First Strand synthesis kit (Takara). Real-time PCR was performed according to the protocol used in our previous study [4]. The expression of targeted genes and tRFs were normalized to GAPDH or U6, respectively. Primers of targeted genes were as follows: human *GAPDH*, forward 5'-GTC TCC TCT GAC TTC AAC AGC G-3' and reverse 5'-ACC ACC CTG TTG CTG TAG CCA A-3'; mouse *GAPDH*, forward 5'-AGG TCG GTG TGA ACG GAT TTG-3' and reverse 5'-TGT AGA CCA TGT AGT TGA GGT CA-3'; human *Alkbh3*, forward 5'-CCA CTG CTA AGA GCC ATC TCC A-3' and reverse 5'-TCA ATC ACT CGT GGC TCA GGA G-3'; mouse *Alkbh3*, forward 5'-AGC CGC ATT GAA GAG AAC ACC AG-3' and reverse 5'-CAT CGT CGC TGT GCC AGT CC-3'. *5'-tRF-GlyGCC*, forward 5'-GGC AGG CGA GAA TTC TAC CAC TGA ACC ACC AA-3'; *5'-half-GlyGCC*, forward 5'-GCA TGG GTG GTT CAG TGG TAG AAT TCT-3'; *5'-half-GluTTC*, forward 5'-TCC CAC ATG GTC TAG CGG TTA GG-3'; *5'-half-LysCTT*, forward 5'-GCC CGG CTA GCT CAG TCG-3'; *i-tRF-ArgCCT*, forward 5'-AGG GAT TGT GGG TTC GAG TCC-3'; and the reverse primer of all the small RNA used the mRQ 3' universal primer.

The quantification of 5'-tRF-GlyGCC

To quantify the absolute amount of *5'-tRF-GlyGCC* in plasma, we established the standard curve for *5'-tRF-GlyGCC* by use of the synthesized standard (Sangon Biotech, Shanghai, China) with the sequence of 5'-GCA UGG GUG GUU CAG UGG UAG AAU UCU CGC C-3'. Setting up 8 concentration gradients of 40, 10, 1, 0.1, 0.01, 0.001, 0.0001, and 0.00001 ng respectively, the standard curve of y-coordinate was the Δ CT value for

each of these concentrations measured by real-time PCR.

For each plasma sample, total RNA was isolated from 125 μ l of plasma (human, BALB/c and BALB/c-nu-nu mice) using the TRIzol LS (Invitrogen) according to the manufacturer's protocol. The small RNA first-strand was generated using the Mir-X™ miRNA First Strand synthesis kit (Takara) according to the manufacturer's protocol in 1 μ l RNA (10 μ l RNA/125 μ l plasma). The Δ CT value of each sample was measured by real-time PCR, and then the amounts of *5'-tRF-GlyGCC* were calculated based on the standard curve (shown in Fig. S1).

Western blot analysis

Western blot analysis was performed as our previously described procedures [40]. The antibodies used in the present study were ALKBH3 (Millipore, BS1236, 1:3000) and GAPDH (BOSTER, BM3876, 1:1000).

Cell line, cell culture, and transfection

Human CRC HCT116, SW620, HCT8, HCT15, SW480, RKO, CaCo2, HT29, Ls578T, cells, normal human colon epithelial cells NCM460, and human monocytic cell line THP-1 were obtained from American Type Culture Collection (Manassas, VA, USA) and maintained in our lab. Non-tumorigenic human peripheral blood B lymphocyte PENG-EBV cells were obtained from Kunming Cell Bank (Chinese Academy of Sciences). The mouse CRC cell CT26 was also purchased from the American Type Culture Collection (Manassas, VA, USA). All cells were maintained in our lab with cultured in RPMI 1640 or DMEM medium (GIBCO, Carlsbad, CA, USA) with 10% fetal bovine serum (FBS) and 1% 100 \times Pen/Strep (Thermo Fisher) in a 5% CO₂ cell culture incubator at 37 °C.

Cell co-culture system was used to evaluate the effects of CRC cells on the expression of *5'-tRF-GlyGCC*. Firstly, blood PENG-EBV or THP-1 cells were plated onto the bottom of a 6-well plate at the density of 2×10^5 cells/well, and CRC cell lines (SW620, HCT116, RKO, SW480, HCT8, and HCT15) were seeded onto the inside of an insert Transwell chamber (polyethylene terephthalate hanging cell culture insert with pore size of 0.4 μ m, Millipore) with a density of 2×10^5 cells/well. Co-culture was started by setting the insert on the 6-well plate. To evaluate the roles of ALKBH3 in the expression of *5'-tRF-GlyGCC*, PENG-EBV and CRC cells (HCT8, HCT15, SW620, RKO, SW480) were transfected with ppB-*Alkbh3* or sh-*Alkbh3* and corresponding vector controls via liposome-mediated transfection.

Animal studies

BALB/c-nu-nu mice and BALB/c mice (4 weeks old) were purchased from Sun Yat-sen University (Guangzhou,

China) Animal Center and raised under pathogen-free conditions. All animal experiments complied with Zhongshan School of Medicine Policy on Care and Use of Laboratory Animals. To establish CRC xenograft model in mice, human CRC cell line HCT116 and mouse CRC cell line CT26 (5×10^6 cells in 150 μ l PBS + 150 μ l Matrigel) were injected into right flanks of BALB/c-nu-nu mice ($n = 6$, male to female = 1:1) and BALB/c mice ($n = 6$, male to female = 1:1), respectively. PBS with 150 μ l was also injected into right flanks of BALB/c-nu-nu mice ($n = 6$, male to female = 1:1) and BALB/c mice ($n = 6$, male to female = 1:1) as the control group, respectively. Mice were euthanized 30 days after cell/PBS injection or if the longest dimension of the tumors reached 20 mm before 30 days. Immediately following euthanasia, blood samples were collected from mice orbit using the tubes for EDTA anticoagulation. Then, 125 μ l blood per sample was used to extract RNA and the remaining blood was further centrifugation to collect plasma.

Statistical analysis

Statistical analysis was performed with IBM SPSS Statistics 15.0, GraphPad Prism version 7.0, and MedCalc version 17.1. Data were reported as mean \pm standard deviation (SD) from at least three independent experiments unless otherwise specified. Data were analyzed by two-tailed unpaired Student's *t* test between two groups and by one-way ANOVA followed by Bonferroni test for multiple comparisons. Spearman correlation test was used for correlation analysis. All statistical tests were two-sided. A *p* value of < 0.05 was considered to be statistically significant. * $p < 0.05$, ** $p < 0.01$, *** $p < 0.001$, **** $p < 0.0001$; ns, no significant.

Results

The expression profiles of tDRs in plasma of CRC and HCs

To investigate the expression profiles of tDRs in plasma of CRC and HCs, small RNAs (smRNA) ranging from 10 to 50 bp from plasma samples of 3 CRC and 3 HC subjects (Table S1) were analyzed using small RNA high-throughput sequencing. The detailed reads data were listed in Table S3. Profiling assay indicated that the abundance of tDRs decreased with the order of 5'-tRF > 5'-half/i-tRF > 3'-tRF > 3'-half in HCs and CRC plasma (Fig. 1a). Further, the proportion of 5'-tRF in CRC plasma was significantly greater than that in HCs (Fig. 1a), suggesting that 5'-tRF might be involved in CRC tumorigenesis and progression. The expression of individual tDR profiles was further analyzed. Hierarchical clustering showed systematic variations in tDR expression in plasma between HCs and CRC (Fig. 1b), and 628 and 745 tDRs were obtained in CRC and HCs, respectively.

The differentially expressed 5'-tRFs in plasma between CRC and HCs were further analyzed. The results showed that the 5'-tRF profiles in CRC plasma were largely different from that in HC plasma (Fig. 1c). For example, the highest abundance 5'-tRF in plasma of HC and CRC was 5'-tRF-*HisGTG* and 5'-tRF-*GlyGCC*, respectively. The expression of 5'-tRF-*GlyGCC*, which accounted for 7.44% of 5'-tRF in HC plasma, increased to 52.24% of 5'-tRF in CRC plasma. In addition, the proportions of 5'-tRF-*GlyCCC* markedly increased in CRC plasma; however, the percentage of 5'-tRF-*HisGTG* and 5'-tRF-*AlaTGC* obviously decreased in CRC plasma (Fig. 1c). All these data suggested that the profiles of 5'-tRFs in CRC plasma were significantly different from that in HCs.

Among the 628 and 745 tDRs identified in CRC and HCs, there were 85 and 202 unique tDRs for each group, respectively (Fig. 1d). Further, 81 tDRs were significantly increased in plasma of CRC than that in HCs (Fig. 1d). To validate the findings of small RNA sequencing, the 5 upregulated candidate tDRs in the above same 3 CRC and 3 HC subjects plasma samples were further checked by qRT-PCR. As showed in Fig. 1e, all measured tDRs in CRC plasma increased compared to that of HCs, while the increase of 5'-tRF-*GlyGCC* was the highest among the five measured ones. All these data revealed that expression profiles of tDRs were varied in plasma of CRC as compared with that in HCs; further, 5'-tRF, particularly 5'-tRF-*GlyGCC*, were significantly increased in CRC plasma.

The levels of 5'-tRF-*GlyGCC* in plasma of CRC patients

5'-tRF-*GlyGCC* located at chromosomes 1, 2, 6, 16, and 17 with a transcript length of 31 nt, and the sequence is 5'-GCA UGG GUG GUU CAG UGG UAG AAU UCU CGC C-3' (MINTbase Unique ID: tRF-35-PNR8YP9LON4VN1). The small RNA-seq data suggested that the 5'-tRF-*GlyGCC* increased in CRC patients was greater than that of other tDRs. Consistently, 5'-tRF-*GlyGCC* was one of the most abundant tDRs detected in human cells and tissues in our previous study [4]. We therefore further checked its expression in plasma of patients with CRC ($n = 105$) and HCs ($n = 90$). Our data showed that the abundance of 5'-tRF-*GlyGCC* was significantly higher in CRC patients than in HCs ($p < 0.0001$, Fig. 2a). We then analyzed the expression of 5'-tRF-*GlyGCC* in different pathological stages of CRC patients (stage I, $n = 11$; stage II, $n = 34$; stage III, $n = 32$; stage IV, $n = 25$). The results showed that the amount of 5'-tRF-*GlyGCC* at each stage of CRC was higher than of HCs ($p < 0.0001$, Fig. 2b). The results indicated that 5'-tRF-*GlyGCC* might be a promising biomarker for the diagnosis of CRC patients.

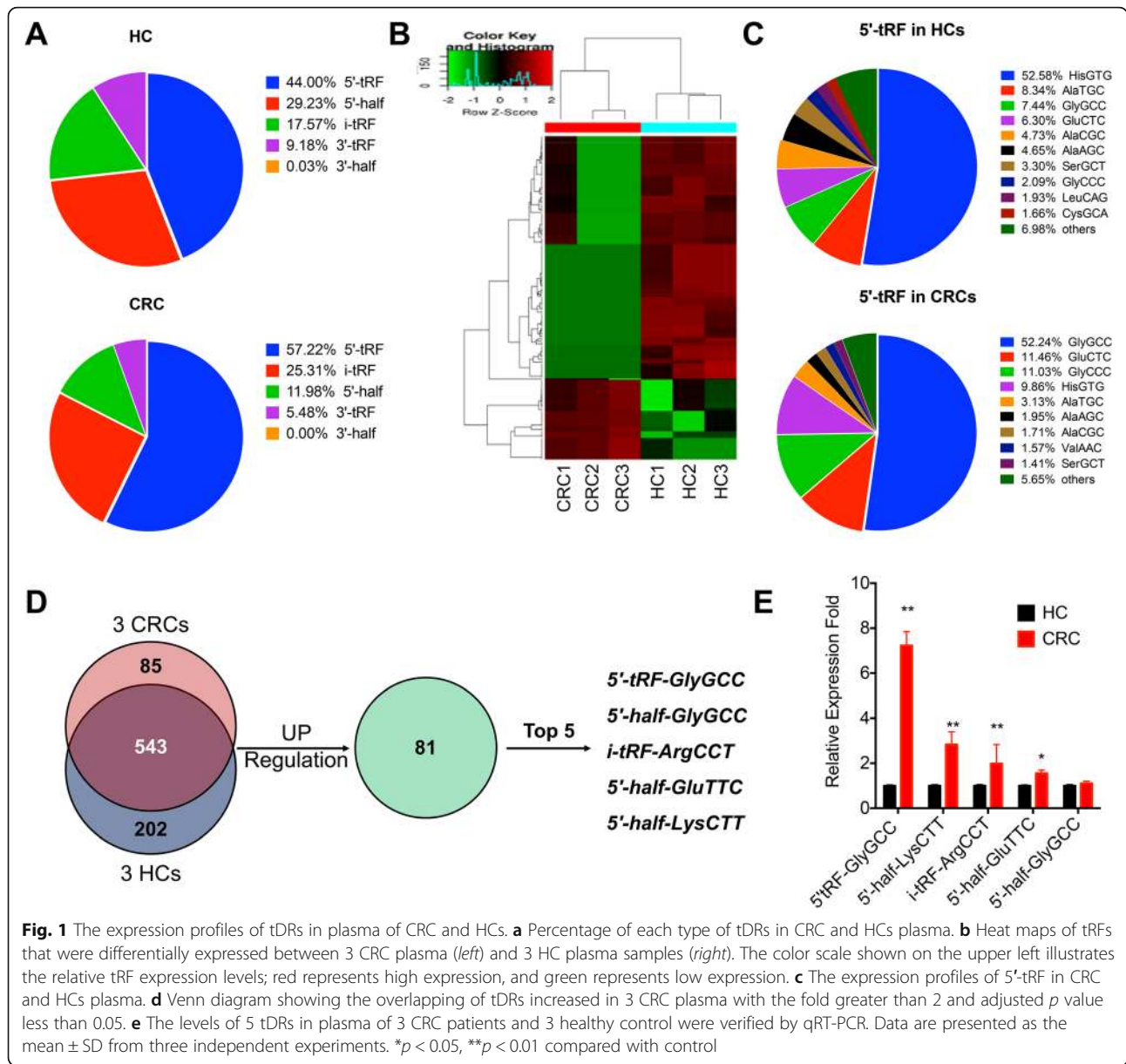


Fig. 1 The expression profiles of tDRs in plasma of CRC and HCs. **a** Percentage of each type of tDRs in CRC and HCs plasma. **b** Heat maps of tRFs that were differentially expressed between 3 CRC plasma (left) and 3 HC plasma samples (right). The color scale shown on the upper left illustrates the relative tRF expression levels; red represents high expression, and green represents low expression. **c** The expression profiles of 5'-tRF in CRC and HCs plasma. **d** Venn diagram showing the overlapping of tDRs increased in 3 CRC plasma with the fold greater than 2 and adjusted *p* value less than 0.05. **e** The levels of 5 tDRs in plasma of 3 CRC patients and 3 healthy control were verified by qRT-PCR. Data are presented as the mean ± SD from three independent experiments. **p* < 0.05, ***p* < 0.01 compared with control

We further evaluated the expression of 5'-tRF-GlyGCC with the progression of CRC. The 5'-tRF-GlyGCC expression was observed to increase as CRC progressed (Fig. 2b). In addition, the abundance of 5'-tRF-GlyGCC in stage I/II CRC patients was significantly less than that in stage III/IV patients (Fig. 2c). Moreover, metastasized CRC patients had significantly higher levels of 5'-tRF-GlyGCC in plasma than those of no metastasis group (*p* < 0.05, Fig. 2d). Also, CRC patients with CEA ≥ 5 ng/ml had significantly greater levels of 5'-tRF-GlyGCC than that of patients with CEA < 5 ng/ml (Fig. 2e). Further, CRC patients with CA199 ≥ 37 IU/ml had significantly greater levels of 5'-tRF-GlyGCC than that of CA199 < 37 IU/ml ones (Fig. 2f). In addition, results showed that the levels of

5'-tRF-GlyGCC in plasma were significantly positively correlated with the levels of CEA (Fig. 2g) and CA199 (Fig. 2h) for CRC patients. However, the distribution of 5'-tRF-GlyGCC in CRC patients seems to be independent of the statuses of gender, age, colon or rectal location, KRAS mutation, MSI/MSS, Ki67, CA125, CA15-3, or FAP expression (Summarized in the Table S4). The results showed that 5'-tRF-GlyGCC was upregulated in plasma of CRC patients and increased with the progression and metastasis of CRC.

Further, we checked whether there was a correlation between the expression of 5'-tRF-GlyGCC in CRC tissues and plasma of the same patients by collection of 16 paired tumor tissues and plasma samples. The results

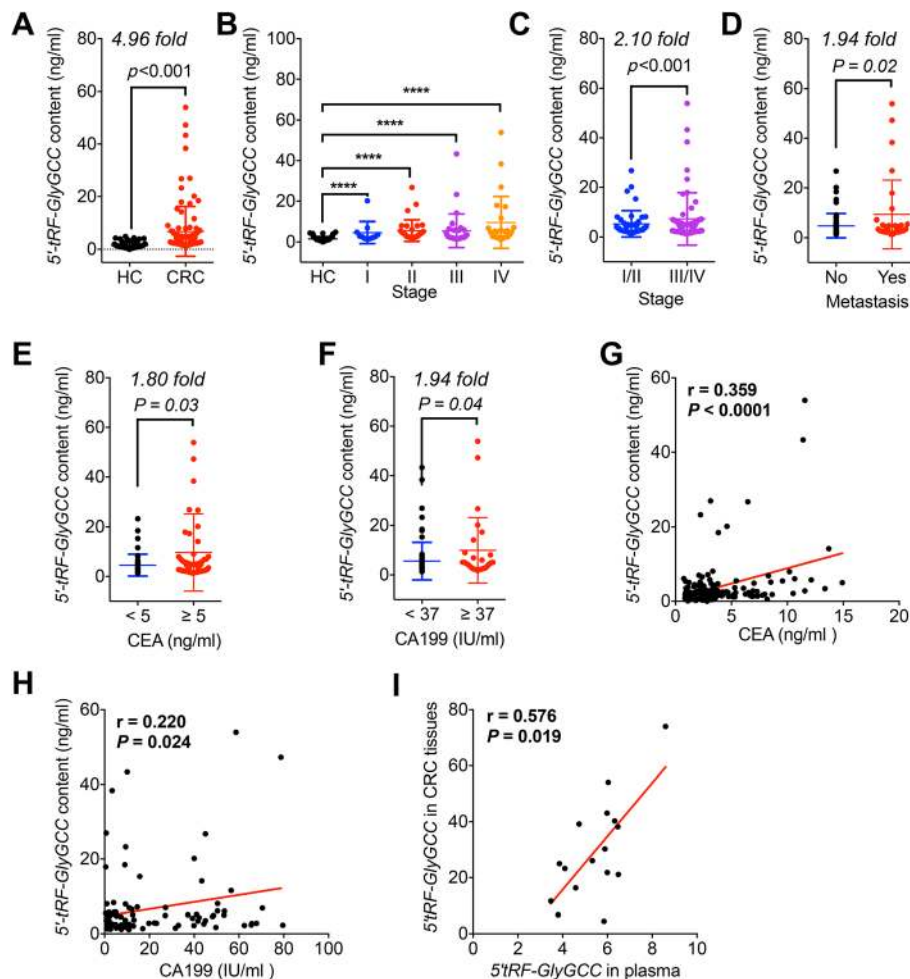


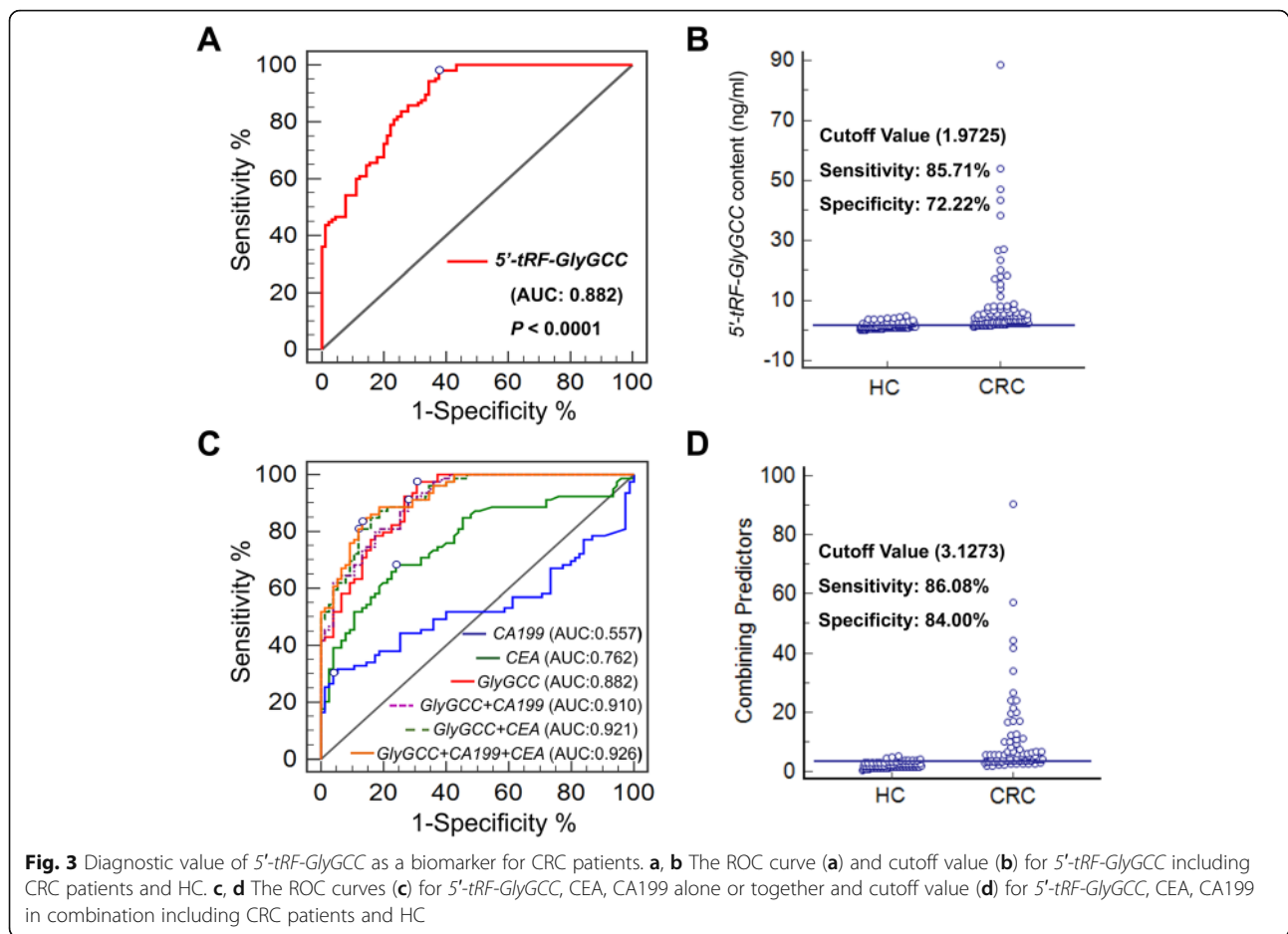
Fig. 2 The levels of 5'-tRF-GlyGCC in plasma of CRC patients. **a** The amount and relative fold of 5'-tRF-GlyGCC in plasma of CRC patients ($n = 105$) and HC ($n = 90$). **b** The amount of 5'-tRF-GlyGCC in plasma of different pathological stages of CRC patients (stage I, $n = 11$; stage II, $n = 34$; stage III, $n = 32$; stage IV, $n = 25$). **c** The comparison of 5'-tRF-GlyGCC levels in plasma of stage I/II ($n = 45$) and III/IV ($n = 57$) CRC patients. **d** The comparison of 5'-tRF-GlyGCC levels in plasma of CRC patients with ($n = 30$) or without ($n = 64$) metastasis. **e** The comparison of 5'-tRF-GlyGCC levels in plasma of CRC patients with CEA ≥ 5 ng/ml ($n = 54$) or CEA < 5 ng/ml ($n = 47$). **f** The comparison of 5'-tRF-GlyGCC levels in plasma of CRC patients with CA199 ≥ 37 IU/ml ($n = 27$) or CA199 < 37 IU/ml ($n = 74$). **g, h** The Spearman correlation of 5'-tRF-GlyGCC amount with the levels of CEA (**g**) or CA199 (**h**) in CRC patients. **i** The Spearman correlation of 5'-tRF-GlyGCC amount in paired plasma and tumor tissues from 16 CRC patients. * $p < 0.05$, ** $p < 0.01$, *** $p < 0.001$, **** $p < 0.0001$

showed that the expression of 5'-tRF-GlyGCC in plasma was significantly correlated with that in the paired CRC tissues (Fig. 2i). It indicated that patients with greater levels of 5'-tRF-GlyGCC in plasma also had higher levels of 5'-tRF-GlyGCC in CRC tissues.

Diagnostic value of 5'-tRF-GlyGCC as a biomarker for CRC patients

To test whether plasma 5'-tRF-GlyGCC levels had diagnostic value for CRC patients, a receiver-operating characteristic (ROC) curve was plotted to identify a cutoff value. As

shown in Fig. 3a and Table S5, plasma 5'-tRF-GlyGCC content could distinguish CRC patients from HCs, with an area under the curve (AUC) of 0.882 (95% CI 0.83 to 0.92, $p < 0.0001$). The optimal cutoff value for 5'-tRF-GlyGCC was 1.9725 (sensitivity 86%, specificity 72%) (Fig. 3b). The results showed that the diagnosis value of 5'-tRF-GlyGCC was much better than that of CEA (AUC 0.762) or CA199 (0.557). Further, the ROC curves of the combination of 5'-tRF-GlyGCC, CEA, and CA199 improved the AUC value to 0.926 (95% CI 0.87–0.96, $p < 0.0001$) (Fig. 3c). The combining optimal cutoff value was 3.1273 (sensitivity 86%,



specificity 84%) (Fig. 3d). This indicated that the plasma levels of *5'-tRF-GlyGCC* provided excellent diagnostic capabilities for CRC patients.

ALKBH3 is involved in the biogenesis of *5'-tRF-GlyGCC*

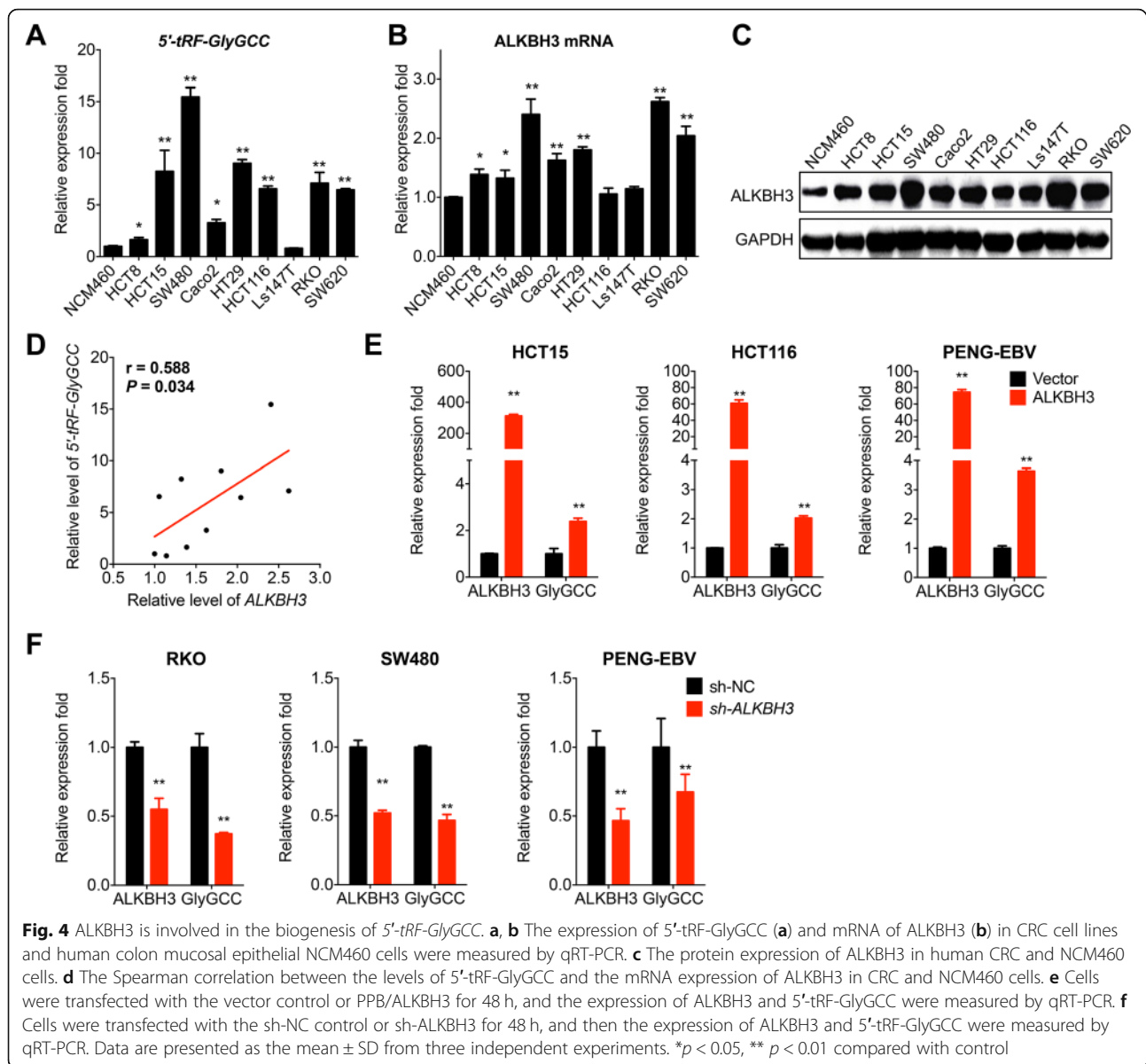
Our previous study reported that ALKBH3 was a tRNA demethylase and has only been identified as inducing the generation of tDRs [4]. We then investigated whether ALKBH3 was involved in the biogenesis of *5'-tRF-GlyGCC*. Firstly, the expression of *5'-tRF-GlyGCC* and ALKBH3 were measured in nine human CRC cell lines and human colon mucosal epithelial cells NCM460. The results showed that both *5'-tRF-GlyGCC* (Fig. 4a) and ALKBH3 mRNA (Fig. 4b) in most measured CRC cell lines was significantly greater than that in NCM460 cells. Consistently, western blot analysis confirmed that the protein expression of ALKBH3 was upregulated in CRC cells (Fig. 4c). Further, the expression of *5'-tRF-GlyGCC* was significantly and positively correlated with the mRNA levels of ALKBH3 in the measured CRC cells (Fig. 4d).

Further, we then overexpressed ALKBH3 in HCT15, HCT116 (ALKBH3 low CRC cells), and blood PENG-

EBV cells via transient transfection (Fig. S2A). The results showed that over expression of ALKBH3 can increase the expression of *5'-tRF-GlyGCC* in all examined cells (Fig. 4 E). We knocked down the expression of ALKBH3 in CRC cell SW480, RKO (ALKBH3 high expression CRC cells), and PENG-EBV cells (Fig. S2B). The results showed that ALKBH3 silencing downregulated the level of *5'-tRF-GlyGCC* in SW480, RKO, and PENG-EBV cells (Fig. 4f). Consistently, overexpression of ALKBH3 in RKO and SW480 cells can increase the expression of *5'-tRF-GlyGCC* (Fig. S4 C), while knock-down the expression of ALKBH3 can decrease the expression of *5'-tRF-GlyGCC* in HCT15 and HCT116 cells (Fig. S4 D). Collectively, our data showed that the tRNA demethylase ALKBH3 was involved in the biogenesis of *5'-tRF-GlyGCC* in both CRC and blood cells.

Co-culture with CRC cells increased *5'-tRF-GlyGCC* of blood cells via ALKBH3

We further investigated the potential mechanisms responsible for upregulation of *5'-tRF-GlyGCC* in plasma of CRC patients. Since circulating tumor cells are widespread in the peripheral blood of CRC patients [9, 25],



we then used Transwell chamber (pore size of 0.45 μm) to establish a co-culture system of peripheral blood cells PENG-EBV and human monocytic cell THP-1 with CRC cells, respectively. Our data showed that co-culture with all examined CRC cells can significantly increase the 5'-tRF-GlyGCC levels in PENG-EBV cells (Fig. 5a). Consistently, co-culture with CRC cells can significantly increase the 5'-tRF-GlyGCC levels in THP-1 cells (Fig. 5b). In addition, when co-cultured with all CRC cells, the mRNA expression of ALKBH3 in PENG-EBV cells also increased significantly (Fig. 5c). Further, western blot analysis confirmed that co-culture with CRC cells increased the protein expression of ALKBH3 in PENG-EBV cells (Fig. 5d). The culture medium of CRC cells could also induce the

expression of 5'-tRF-GlyGCC in both PENG-EBV and THP-1 cells while the boiled medium (100 $^{\circ}\text{C}$ for 5 min) had no similar effect (data not shown), which suggested the CRC secreted cytokines or other substances can induce expression of 5'-tRF-GlyGCC.

We further investigated whether ALKBH3 is involved in CRC-induced 5'-tRF-GlyGCC of blood cells. The expression of ALKBH3 was knocked down in PENG-EBV cells (Fig. 5e). The results showed that the deletion of ALKBH3 can attenuate expression of 5'-tRF-GlyGCC in PENG-EBV cells induced by SW620 (Fig. 5f) and SW480 (Fig. 5g). It suggested that CRC cells can increase the 5'-tRF-GlyGCC levels in peripheral blood cells via upregulation of ALKBH3.

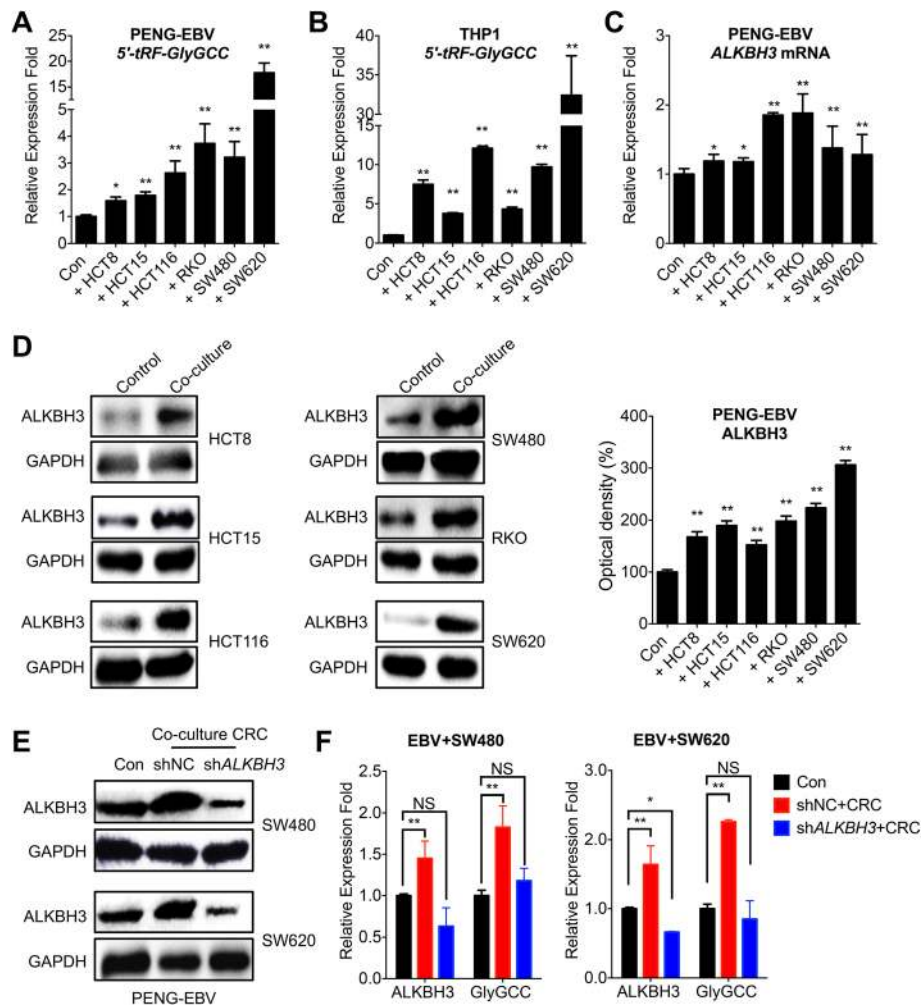


Fig. 5 Co-culture with CRC cells increased 5'-tRF-GlyGCC of blood cells via ALKBH3. **a, b** The levels of 5'-tRF-GlyGCC in PENG-EBV (**a**) or THP-1 (**b**) cells co-cultured with or without CRC cells was tested by RT-PCR. **c** The levels of ALKBH3 mRNA in PENG-EBV cells co-cultured with or without CRC cells were tested by RT-PCR. **d** The protein levels of ALKBH3 in PENG-EBV cells co-cultured with or without CRC cells were checked by western blot analysis and quantitatively analyzed. **e, f** PENG-EBV cells pre-transfected with sh-control or sh-ALKBH3 were further co-cultured with or without CRC cells for 48 h; the expression of ALKBH3 **e** and 5'-tRF-GlyGCC **f** in PENG-EBV cells were checked. Data are presented as the mean \pm SD from three independent experiments. * $p < 0.05$, ** $p < 0.01$ compared with control; NS, no significant

Xenografted CRC tumors increased levels of 5'-tRF-GlyGCC in plasma of mice

To evaluate the in vivo effects of CRC tumors on 5'-tRF-GlyGCC expression, we established the human CRC HCT116 xenografts by using of BALB/c-nu-nu mice ($n = 6$, male to female = 1:1, Fig. S3A). Our data showed that the plasma levels of 5'-tRF-GlyGCC significantly increased in xenografted nude mice as compared to those in the control group ($p < 0.05$, Fig. 6a). Further, the mRNA expression of ALKBH3 in peripheral blood significantly increased ($p < 0.01$, Fig. 6b). Then, mouse CRC CT26 cells were used to establish xenografts with BALB/c mice ($n = 6$, male to female = 1:1, Fig. S3B). Consistently, the plasma levels of 5'-tRF-GlyGCC (Fig. 6c) and the mRNA expression of ALKBH3 in peripheral blood

(Fig. 6d) significantly ($p < 0.05$) increased in CT26 xenografted BALB/c mice. In addition, the expression of 5'-tRF-GlyGCC level was significantly and positively associated with the expression of ALKBH3 in tumor-bearing mice (Fig. 6e). These results indicated that CRC xenograft can promote plasma levels of 5'-tRF-GlyGCC, accompanied by the up-regulation of ALKBH3 in vivo.

Discussion

The detection of precursor lesions and early-onset CRC is critical for prevention and therapy of this disease. Colonoscopy is considered as the gold standard for CRC screening; however, it is invasive, expensive, and has low compliance rates and complications such as hemorrhage and perforation [22]. While the most commonly used

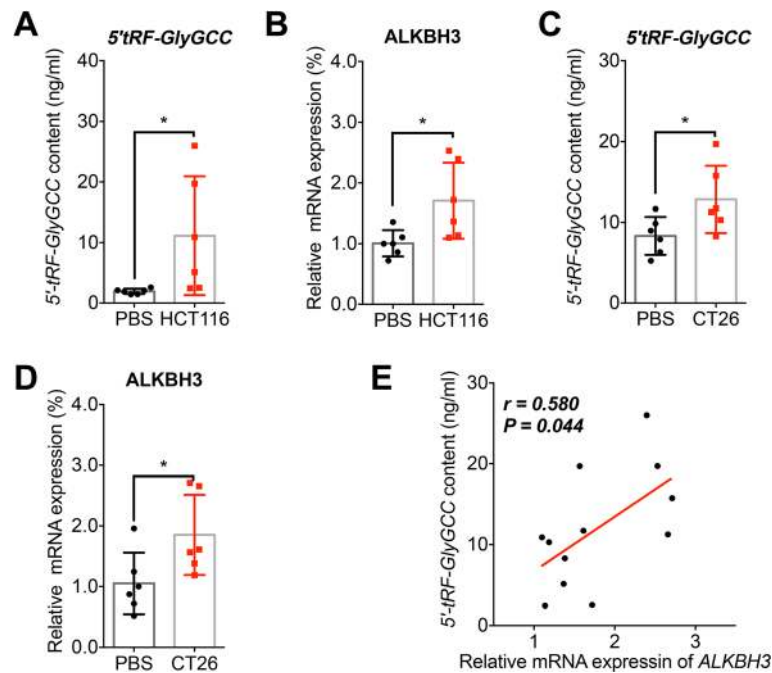


Fig. 6 Xenografted CRC tumors increased levels of 5'-tRF-GlyGCC in plasma of mice. **a** Levels of 5'-tRF-GlyGCC in plasma of nude mice of control ($n = 6$) or bearing human CRC HCT116 tumor ($n = 6$). **b** Relative mRNA level of ALKBH3 in nude mice blood of control ($n = 6$) or bearing human CRC HCT116 tumor ($n = 6$). **c** Levels of 5'-tRF-GlyGCC in plasma of BALB/c mice of control ($n = 6$) or bearing mouse CRC CT26 tumor ($n = 6$). **d** Relative mRNA level of ALKBH3 in BALB/c mice blood control ($n = 6$) or bearing mouse CRC CT26 tumor ($n = 6$). **e** The Spearman correlation between the levels of 5'-tRF-GlyGCC and the mRNA expression of ALKBH3 in xenografted mice. * $p < 0.05$ as compared with the PBS group

non-invasive screening tests such as fecal OB testing and fecal immunochemical test (FIT) have lower sensitivity and specificity [34], there is an imperative need to develop novel and robust non-invasive strategies for CRC diagnosis. Further, biomarkers that enable the proper selection of patients would be helpful for the improvement of therapy efficiency. In this study, we found that plasma level of 5'-tRF-GlyGCC could be a novel biomarker to screen for CRC. In addition, the combination with the current tumor markers such as CEA and CA199 can further enhance its diagnostic values.

With the development of sequencing technology, emerging evidence revealed that dysregulation of tDRs was involved in the progression of human diseases, such as cancer, neurodegenerative diseases, and inherited metabolic disorders [8, 11, 28, 33]. Among the few tDRs that have been functionally characterized, tRF/miR-1280, a 17-nt fragment derived from tRNA^{Leu} and pre-miRNA, suppressed CRC growth and metastasis [12]. Enriched 5'-tiRNA-Val was observed in CRC patients and correlated with tumor metastasis [19]. Also, several recent studies have revealed that tDRs were non-invasive diagnostic biomarkers for various diseases including cancer [7, 10, 31, 43].

By small RNA sequencing, we identified that the profile of tDRs in plasma of CRC was significantly different

from that of HCs. This is particularly true for the expression of 5'-tRF and 5'-tRF-GlyGCC, whose levels significantly increased in CRC plasma. The AUC for 5'-tRF-GlyGCC in CRC group was 0.882 (95% CI, 0.83–0.92), which is markedly greater than that of CEA and CA199. The combination of CEA and CA199 with 5'-tRF-GlyGCC improved the AUC to 0.926 (95% CI, 0.87–0.96). It has been revealed that tRF-25, tRF-38, and tRF-18 can be used to diagnose osteoporosis with an average AUC of 0.815 [38]. As to CRC diagnosis, circulating microRNAs can be used as useful non-invasive diagnostic biomarkers with AUC values ranged from 0.6 to 0.9 [2]. However, so far, there is no single stand-alone miRNA that has yet been identified as an ideal biomarker for the diagnosis of CRC [14]. Our data showed for the first time that plasma levels of 5'-tRF-GlyGCC significantly increased in the CRC group as compared to those in the HC group. Further, blood cells co-cultured with CRC cells or mice xenografted with CRC tumors showed increased levels of 5'-tRF-GlyGCC. All these data suggested that 5'-tRF-GlyGCC might be a robust biomarker for CRC diagnosis. Considering that 5'-tRF-GlyGCC has been reported to be critical for the progression of other cancers such as breast [36] and lung [4] cancer, whether it will be used as a biomarker for other cancers requires further study.

We further found that the tRNA demethylase ALKBH3 identified in our previous study [4] was involved in the biogenesis of 5'-tRF-GlyGCC both in vitro and in vivo. The expression of ALKBH3 can positively regulate the generation of 5'-tRF-GlyGCC in blood cells. Further, blood cells co-cultured with CRC cells or mice xenografted with CRC tumors can increase the biogenesis of 5'-tRF-GlyGCC via an ALKBH3-dependent manner. ALKBH3 has been suggested to function as a DNA-repair protein to protect genomic integrity [5, 39]. Our previous study has revealed that it can specifically demethylate m¹A and m³C of tRNA to induce the generation of tDRs [4]. In addition, ALKBH3 is highly expressed in various cancers [29, 32] to trigger the cancer progression via induction of tDRs [4]. Also, ALKBH3 is suggested to be beneficial to the growth and progression of CRC cells [20]. The role of tDRs including 5'-tRF-GlyGCC in the promotion effects of ALKBH3 on cancer progression needs further study.

Conclusions

We showed that the profile and abundance of tDRs in the plasma of CRC patients and highlighted that 5'-tRF-GlyGCC is a promising biomarker for CRC diagnosis. Moreover, we found high levels of 5'-tRF-GlyGCC in CRC might be due to the upregulation of tRNA demethylases ALKBH3 by analyzing data from cellular, tumor bearing mice. It should be noted that the composition of tDRs might be different in different tumor models; the role of 5'-tRF-GlyGCC as a biomarker and its carcinogenesis in other types of cancer need further investigation.

Supplementary Information

The online version contains supplementary material available at <https://doi.org/10.1186/s13073-021-00833-x>.

Additional file 1: Fig. S1. The standard curve of 5'-tRF-GlyGCC quantification. **Fig. S2.** ALKBH3 is involved in the biogenesis of 5'-tRF-GlyGCC. **Fig. S3.** The nude mice (A) and BALB/c (B) mice bearing CRC cells xenografted tumor. **Table S1.** Background information of the Small RNA sequencing samples. **Table S2.** Background demographic of the study cohorts. **Table S4.** Relationship between the levels of 5'-tRF-GlyGCC and the clinicopathological variables in CRC patients. **Table S5.** Clinical diagnosis utility about various marker alone and their combination effects for CRC diagnosis.

Additional file 2: Supplemental Table S3. The detailed reads data of tDRs in plasma of CRC and HCs.

Abbreviations

ALKBH3: AlkB homolog 3; AUC: Area under the curve; CA: Carbohydrate antigen; CEA: Carcinoembryonic antigen; CRC: Colorectal cancer; EDTA: Ethylene diamine tetraacetic acid; FBS: Fetal bovine serum; FIT: Fecal immunochemical test; GAPDH: Glyceraldehyde-3-phosphate dehydrogenase; HC: Healthy controls; m¹A: 1-Methyladenosine; m¹G: 1-Methylguanosine; m^{2,2}G: 2,2-Dimethylguanosine; m³C: 3-Methylcytidine; OB: Occult blood; PP: Polypropylene; qRT-PCR: Quantitative real-time PCR; ROC: The receiver-operating characteristic; SD: Standard deviation; smRNAs: Small RNAs;

tDRs: tRNA-derived small RNAs; tRFs: tRNA-derived small RNA fragments; tRNA: Transfer RNA

Acknowledgements

We thank Prof. Chuan He at the Department of Chemistry, the University of Chicago, for discussion. We thank Kawo Chan at the Guangdong Institute of Gastroenterology, The Sixth Affiliated Hospital, Sun Yat-sen University, for proofreading.

Authors' contributions

Conception and design: Yingmin Wu, Xiangling Yang, Guanmin Jiang, Huanliang Liu, Hongsheng Wang; acquisition of data: Yingmin Wu, Xiangling Yang, Guanmin Jiang, Haisheng Zhang, Lichen Ge, Feng Chen, Jiexin Li; analysis and interpretation of data: Yingmin Wu, Xiangling Yang, Guanmin Jiang, Lichen Ge, Feng Chen, Hongsheng Wang; writing, review, and/or revision of the manuscript: Yingmin Wu, Xiangling Yang, Jiexin Li, Hongsheng Wang. The authors read and approved the final manuscript.

Authors' information

Not applicable

Funding

This research was supported by the National Natural Science Foundation of China (Grant Nos. 81973343, 81672413, 82072365, and 31801197), the Open Program of Shenzhen Bay Laboratory (No. SZBL202009051006), the Guangdong Provincial Key Laboratory of Chiral Molecule and Drug Discovery (2019B030301005), the Guangdong Provincial Key Laboratory of Construction Foundation (No. 2017B030314030), the Fundamental Research Funds for the Central Universities (Sun Yat-sen University) (Nos.19ykpy130 and 19ykzd24), the Guangdong Basic and Applied Basic Research Foundation (No. 2020A1515010290), and the China Postdoctoral Science Foundation (No. 2018 M643354, 2020 T130751).

Availability of data and materials

All data generated or analyzed during this study are included in this published article and its Additional files.

Ethics approval and consent to participate

For all of the patients who participated in this study, written informed consent was obtained. It was approved by the Ethical Committee of Sun Yat-sen University according to the Chinese Ethical Regulations and conducted according to the guidelines of the Declaration of Helsinki. All animal experiments complied with the Zhongshan School of Medicine Policy on the Care and Use of Laboratory Animals.

Consent for publication

The authors confirmed that we have obtained written consent from the patient to publish the manuscript.

Competing interests

The authors declare that they have no competing interests.

Author details

¹Guangdong Key Laboratory of Chiral Molecule and Drug Discovery, School of Pharmaceutical Sciences, Sun Yat-sen University, Guangzhou 510006, Guangdong, China. ²Guangdong Provincial Key Laboratory of Colorectal and Pelvic Floor Diseases, Guangdong Institute of Gastroenterology, The Sixth Affiliated Hospital, Sun Yat-sen University, Guangzhou 510655, Guangdong, China. ³Department of Clinical Laboratory, The Sixth Affiliated Hospital, Sun Yat-sen University, Guangzhou 510655, Guangdong, China. ⁴Department of Clinical Laboratory, The Fifth Affiliated Hospital, Sun Yat-sen University, Zhuhai 519000, Guangdong, China. ⁵Department of Clinical Laboratory, Jinling Hospital, Medical School of Nanjing University, Nanjing 210002, China.

Received: 4 March 2020 Accepted: 14 January 2021

Published online: 09 February 2021

References

- Borek E, Baliga BS, Gehrke CW, Kuo CW, Belman S, Troll W, Waalkes TP. High turnover rate of transfer RNA in tumor tissue. *Cancer Res.* 1977;37:3362–6.

2. Carter JV, Galbraith NJ, Yang DY, Burton JF, Walker SP, Galandiuk S. Blood-based microRNAs as biomarkers for the diagnosis of colorectal cancer: a systematic review and meta-analysis. *Br J Cancer*. 2017;116:762–74.
3. Chen Q, Yan M, Cao Z, Li X, Zhang Y, Shi J, Feng GH, Peng H, Zhang X, Zhang Y, et al. Sperm tsRNAs contribute to intergenerational inheritance of an acquired metabolic disorder. *Science*. 2016;351:397–400.
4. Chen Z, Qi M, Shen B, Luo G, Wu Y, Li J, Lu Z, Zheng Z, Dai Q, Wang H. Transfer RNA demethylase ALKBH3 promotes cancer progression via induction of tRNA-derived small RNAs. *Nucleic Acids Res*. 2019;47:2533–45.
5. Dango S, Mosammaparast N, Sowa ME, Xiong LJ, Wu F, Park K, Rubin M, Gygi S, Harper JW, Shi Y. DNA unwinding by ASCC3 helicase is coupled to ALKBH3-dependent DNA alkylation repair and cancer cell proliferation. *Mol Cell*. 2011;44:373–84.
6. Das V, Kalita J, Pal M. Predictive and prognostic biomarkers in colorectal cancer: a systematic review of recent advances and challenges. *Biomed Pharmacother*. 2017;87:8–19.
7. Feng WT, Li YF, Chu JH, Li J, Zhang YH, Ding XR, Fu ZY, Li W, Huang X, Yin YM. Identification of tRNA-derived small noncoding RNAs as potential biomarkers for prediction of recurrence in triple-negative breast cancer. *Cancer Med-U.S.* 2018;7:5130–44.
8. Goodarzi H, Liu X, Nguyen HC, Zhang S, Fish L, Tavazoie SF. Endogenous tRNA-derived fragments suppress breast cancer progression via YBX1 displacement. *Cell*. 2015;161:790–802.
9. Hamm A, Prenen H, Van Delm W, Di Matteo M, Wenes M, Delamarre E, Schmidt T, Weitz J, Sarmiento R, Dezi A, et al. Tumour-educated circulating monocytes are powerful candidate biomarkers for diagnosis and disease follow-up of colorectal cancer. *Gut*. 2016;65:990–1000.
10. Hogg MC, Raouf R, El Naagar H, Monsefi N, Delanty N, O'Brien DF, Bauer S, Rosenow F, Henshall DC, Prehn JHM. Elevation of plasma tRNA fragments precedes seizures in human epilepsy. *J Clin Investig*. 2019;129:2946–51.
11. Honda S, Loher P, Shigematsu M, Palazzo JP, Suzuki R, Imoto I, Rigoutsos I, Kirino Y. Sex hormone-dependent tRNA halves enhance cell proliferation in breast and prostate cancers. *Proc Natl Acad Sci U S A*. 2015;112:E3816–25.
12. Huang B, Yang H, Cheng X, Wang D, Fu S, Shen W, Zhang Q, Zhang L, Xue Z, Li Y, et al. tRF/miR-1280 suppresses stem cell-like cells and metastasis in colorectal cancer. *Cancer Res*. 2017;77:3194–206.
13. Huang Y, Ge H, Zheng MJ, Cui YY, Fu ZY, Wu XW, Xia YQ, Chen LE, Wang ZH, Wang S, Xie H. Serum tRNA-derived fragments (tRFs) as potential candidates for diagnosis of nontriple negative breast cancer. *J Cell Physiol*. 2020;235:2809–24.
14. Jung G, Hernandez-Illan E, Moreira L, Balaguer F, Goel A. Epigenetics of colorectal cancer: biomarker and therapeutic potential. *Nat Rev Gastro Hepat*. 2020;17:111–30.
15. Kim HK, Fuchs G, Wang S, Wei W, Zhang Y, Park H, Roy-Chaudhuri B, Li P, Xu J, Chu K, et al. A transfer-RNA-derived small RNA regulates ribosome biogenesis. *Nature*. 2017;552:57–62.
16. Kumar P, Mudunuri SB, Anaya J, Dutta A. tRFdb: a database for transfer RNA fragments. *Nucleic Acids Res*. 2015;43:D141–5.
17. Lee YS, Shibata Y, Malhotra A, Dutta A. A novel class of small RNAs: tRNA-derived RNA fragments (tRFs). *Genes Dev*. 2009;23:2639–49.
18. Li HB, Tong J, Zhu S, Batista PJ, Duffy EE, Zhao J, Bailis W, Cao G, Kroehling L, Chen Y, et al. m(6A) mRNA methylation controls T cell homeostasis by targeting the IL-7/STAT5/SOCS pathways. *Nature*. 2017;548:338–42.
19. Li SQ, Shi XL, Chen MX, Xu NQ, Sun DS, Bai R, Chen HY, Ding KF, Sheng JH, Xu ZP. Angiogenin promotes colorectal cancer metastasis via tRNA production. *Int J Cancer*. 2019;145:1395–407.
20. Luo J, Emanuele MJ, Li DN, Creighton CJ, Schlabach MR, Westbrook TF, Wong KK, Elledge SJ. A genome-wide RNAi screen identifies multiple synthetic lethal interactions with the Ras oncogene. *Cell*. 2009;137:835–48.
21. Okugawa Y, Grady WM, Goel A. Epigenetic alterations in colorectal cancer: emerging biomarkers. *Gastroenterology*. 2015;149:1204.
22. Quintero E, Castells A, Bujanda L, Cubiella J, Salas D, Lanás A, Andreu M, Carballo F, Morillas JD, Hernandez C, et al. Colonoscopy versus fecal immunochemical testing in colorectal-cancer screening. *N Engl J Med*. 2012;366:697–706.
23. Ribeiro MS, Wallace MB. Endoscopic treatment of early cancer of the colon. *Gastroenterol Hepatol (N Y)*. 2015;11:445–52.
24. Samadder NJ, Curtin K, Tuohy TM, Pappas L, Boucher K, Provenzale D, Rowe KG, Mineau GP, Smith K, Pimentel R, et al. Characteristics of missed or interval colorectal cancer and patient survival: a population-based study. *Gastroenterology*. 2014;146:950–60.
25. Sastre J, Maestro ML, Puente J, Veganzones S, Alfonso R, Rafael S, Garcia-Saenz JA, Vidaurreta M, Martin M, Arroyo M, et al. Circulating tumor cells in colorectal cancer: correlation with clinical and pathological variables. *Ann Oncol*. 2008;19:935–8.
26. Schorn AJ, Gutbrod MJ, LeBlanc C, Martienssen R. LTR-retrotransposon control by tRNA-derived small RNAs. *Cell*. 2017;170(61–71):e11.
27. Schuber F, Pinck M. On the chemical reactivity of aminoacyl-tRNA ester bond. 2. Aminolysis by tris and diethanolamine. *Biochimie*. 1974;56:391–5.
28. Sharma U, Conine CC, Shea JM, Boskovic A, Derr AG, Bing XY, Belleannee C, Kucukural A, Serra RW, Sun F, et al. Biogenesis and function of tRNA fragments during sperm maturation and fertilization in mammals. *Science*. 2016;351:391–6.
29. Shimada K, Fujii T, Tsujikawa K, Anai S, Fujimoto K, Konishi N. ALKBH3 contributes to survival and angiogenesis of human urothelial carcinoma cells through NADPH oxidase and tweak/Fn14/VEGF signals. *Clin Cancer Res*. 2012;18:5247–55.
30. Siegel RL, Miller KD, Jemal A. Cancer statistics, 2016. *CA Cancer J Clin*. 2016;66:7–30.
31. Sun C, Fu Z, Wang S, Li J, Li Y, Zhang Y, Yang F, Chu J, Wu H, Huang X, et al. Roles of tRNA-derived fragments in human cancers. *Cancer Lett*. 2018;414:16–25.
32. Tasaki M, Shimada K, Kimura H, Tsujikawa K, Konishi N. ALKBH3, a human ALKB homologue, contributes to cell survival in human non-small-cell lung cancer. *Br J Cancer*. 2011;104:700–6.
33. Thompson DM, Parker R. Stressing out over tRNA cleavage. *Cell*. 2009;138:215–9.
34. Tinmouth J, Lansdorp-Vogelaar I, Allison JE. Faecal immunochemical tests versus guaiac faecal occult blood tests: what clinicians and colorectal cancer screening programme organisers need to know. *Gut*. 2015;64:1327–37.
35. Waalkes TP, Gehrke CW, Tormey DC, Zumwalt RW, Hueser JN, Kuo KC, Lakings DB, Ahmann DL, Moertel CG. Urinary excretion of polyamines by patients with advanced malignancy. *Cancer Chemother Rep*. 1975;59:1103–16.
36. Wang XM, Yang YN, Tan XY, Ma XL, Wei D, Yao YF, Jiang P, Mo DP, Wang T, Yan F. Identification of tRNA-derived fragments expression profile in breast cancer tissues. *Curr Genomics*. 2019;20:199–213.
37. Xu WL, Yang Y, Wang YD, Qu LH, Zheng LL. Computational approaches to tRNA-derived small RNAs. *Noncoding RNA*. 2017;3:2.
38. Zhang Y, Cai F, Liu J, Chang HZ, Liu L, Yang AL, Liu XD. Transfer RNA-derived fragments as potential exosome tRNA-derived fragment biomarkers for osteoporosis. *Int J Rheum Dis*. 2018;21:1659–69.
39. Zheng G, Fu Y, He C. Nucleic acid oxidation in DNA damage repair and epigenetics. *Chem Rev*. 2014;114:4602–20.
40. Zhou Y, Lu L, Jiang G, Chen Z, Li J, An P, Chen L, Du J, Wang H. Targeting CDK7 increases the stability of Snail to promote the dissemination of colorectal cancer. *Cell Death Differ*. 2019;26:1442–52.
41. Zhu L, Li J, Gong Y, Wu Q, Tan S, Sun D, Xu X, Zuo Y, Zhao Y, Wei YQ, et al. Exosomal tRNA-derived small RNA as a promising biomarker for cancer diagnosis. *Mol Cancer*. 2019a;18:74.
42. Zhu L, Liu X, Pu W, Peng Y. tRNA-derived small non-coding RNAs in human disease. *Cancer Lett*. 2018;419:1–7.
43. Zhu LW, Li TW, Shen YJ, Yu XC, Xiao BX, Guo JM. Using tRNA halves as novel biomarkers for the diagnosis of gastric cancer. *Cancer Biomarkers*. 2019b;25:169–76.

Publisher's Note

Springer Nature remains neutral with regard to jurisdictional claims in published maps and institutional affiliations.